JOURNAL OF PHYSICAL ORGANIC CHEMISTRY
J. Phys. Org. Chem. 2000; **13:** 654–658

Determining chemical rate coefficients using time-gated fluorescence correlation spectroscopy

Don C. Lamb,[1]* Andreas Schenk,[2] Carlheinz Röcker[2] and G. Ulrich Nienhaus[1,2]

[1]Department of Physics, University of Illinois at Urbana-Champaign, Urbana, Illinois 61801, USA
[2]Department of Biophysics, University of Ulm, D-89069 Ulm, Germany

Received 13 December 1999; revised 20 April 2000; accepted 25 April 2000

ABSTRACT: In recent years, fluorescence correlation spectroscopy (FCS) has become an important technique for studying dynamic processes of molecules in thermodynamic equilibrium. Fluorescent organic molecules are excited by laser light, and the emitted light quanta from a small number of molecules in a volume of ~1 fl are collected using a high numerical aperture microscope objective and photon counting detection. Translational and rotational diffusion, chemical reactions (including photochemistry) and conformational changes of the molecules give rise to temporal correlations in the fluorescence intensity fluctuations that can be revealed by autocorrelation analysis. A method is presented to improve the sensitivity of FCS measurements on samples containing multiple fluorescent species. Using pulsed laser excitation in conjunction with electronic gating in the detection channel, we preferentially suppress the emission from the short lifetime components by fluorescence lifetime separation. We demonstrate the usefulness of this technique by applying it to the binding reaction of the organic dye 1-anilino-8-naphthalenesulfonic acid in the interior of the small globular protein apomyoglobin. When studying this chemical reaction with FCS, a relaxation component appears in the autocorrelation function which can be enhanced by the time gating technique. Furthermore, the analysis is considerably simplified and both kinetic and equilibrium coefficients of the reaction can be determined.

KEYWORDS: time-gated fluorescence correlation spectroscopy; autocorrelation analysis; bimolecular reaction; apomyoglobin; 1-anilino-8-naphthalenesulfonic acid

INTRODUCTION

In recent years, fluorescence correlation spectroscopy (FCS) has become a popular technique for the study of dynamic processes involving fluorescent molecules in solution under thermal equilibrium conditions.[1,2] The method has single-molecule sensitivity and can be used with fluorophore concentrations in the nanomolar to femtomolar range. FCS measures intensity fluctuations of the light emitted by fluorophores in a tiny open volume element created by tight focusing of a laser beam. With high numerical aperture objectives and confocal detection or two-photon excitation, sample volumes as small as 0.2 fl can be achieved. The intensity fluctuations can be caused by translational diffusion in and out of the excitation volume,[3] rotational diffusion within the sample volume,[4] chemical reactions[3,5–7] (e.g. association and dissociation of macromolecules), photochemical reactions[8,9] (such as triplet state excitation), and conformational changes of macromolecules.[10,11]

Whenever a fluorescent molecule enters the sensitive volume, it will be excited by laser light, and fluorescence emission will be registered until it exits again. Hence photons do not arrive purely stochastically in time at the detector, but come in bursts. The slower the molecule diffuses, the longer the burst will last. If the fluorescent molecule undergoes a chemical transformation, its diffusion coefficient may change, for instance by association with another molecule, which will affect the length of the burst. Moreover, the reaction may also affect the intensity or spectral shape of the emitted fluorescence, and thus the intensity measured at the detector may flicker during a burst due to repeated forward and backward reaction steps.

In an FCS experiment, fluorescence quanta and their respective arrival times are collected from many bursts, and the observed fluorescence fluctuations are quantified by statistical analysis, based on the photon counting histogram,[12] fluorescence intensity distribution analysis[13] or correlation functions.[14] Here we will be concerned with the latter approach. The amplitude of the intensity autocorrelation function depends on the average number of fluorescent particles in the volume and hence on the concentration, whereas the correlation

**Correspondence to:* D. C. Lamb, Department of Biophysics, University of Ulm, D-89069 Ulm, Germany.

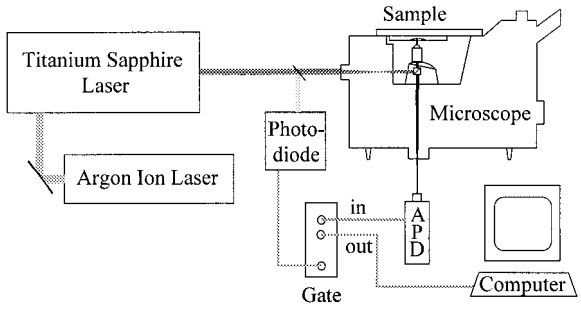

Figure 1. Schematic diagram of the two-photon fluorescence microscope with time-gated detection

times provide information about the time-scales of the intensity fluctuations. Each registered photon, however, carries more information than its arrival time relative to that of other photons. It has a particular energy, polarization and delay time between absorption and emission. This information can give additional insight into the processes under investigation. Here, we present a simple extension of the FCS technique with which we suppress photons based on the delay between excitation and emission. The technique requires a pulsed laser as an excitation source and a laser-synchronized gate in the detection channel. This method allows us to vary the relative contributions of multiple species having different fluorescence lifetimes to the autocorrelation function, which can be useful for a variety of purposes such as rejection of background fluorescence, increase in sensitivity towards a particular fluorescent species and the study of lifetime distributions, which are often observed in the fluorescence emission of biological macromolecules.

EXPERIMENTAL

Sample preparation. All chemicals, unless stated otherwise, were of analytical grade and dissolved in Milli-Q water (Millipore, Milli-Q Plus). Tetramethylrhodamine (TMR) and 1-anilino-8-naphthalenesulfonic acid (ANS) were purchased from Molecular Probes. For the ligand binding studies, horse heart apomyoglobin (apoMb) was purchased from Sigma-Aldrich, dissolved in 10 mM potassium phosphate buffer (pH 7), centrifuged for 15 min at 2800 *g* and room temperature to remove any aggregates or impurities and diluted to a concentration of 300 nM. A stock solution of ANS was made by dissolving the dye in methanol and diluting the mixture by a factor of 100 in buffer (10 mM potassium phosphate, pH 7). A small amount of the concentrated stock solution was added directly to the 300 nM apoMb sample in 10 mM potassium phosphate buffer (pH 7.0) to give a final ANS concentration of 1 μM. For measurement of protein diffusion without ANS ligand binding, myoglobin was stochastically labeled with Oregon Green (Oregon Green 514 carboxylic acid succinimidyl ester, Molecular Probes) according to standard procedures.

Experimental setup. Our FCS setup uses pulsed two-photon excitation, in which two near-infrared photons are absorbed simultaneously to induce an electronic transition in the visible region.[15] A schematic of the apparatus is shown in Fig. 1. It consists of an argon ion laser-pumped Ti:sapphire laser (Coherent, Mira 900), producing 150 fs laser pulses at 76 MHz in the near-infrared region (790 nm), and an epi-illuminated fluorescence microscope (Zeiss, Axiovert 135 TV). The laser was focused into the sample by a water-immersion objective [Zeiss, Plan-Apochromat, 63×, numerical aperture (NA) 1.2]. The resulting fluorescence was collected through the same objective and separated from the laser light by a dichroic mirror (Chroma, 640DCSPXR) and filter (Schott, BG39). The fluorescence was focused on to an avalanche photodiode detector (APD) (EG&G, SPCM-AQ-161) operated in the single photon counting mode. Its output was connected to an autocorrelation card (ALV, ALV5000/E) through an electronic gate.

Fluorescence intensity decays were measured using a time-correlated single photon counting card (PicoQuant, TimeHarp 100). The data were least-squares fitted with a single or double exponential function which was convoluted with the instrumental response function determined independently.

Time gating. The heart of the electronic gate is a fast TTL AND gate. The TTL output of 10 ns width from the APD was compressed to 2 ns and connected to one of the AND gate inputs, and the square pulse output of a high-frequency pulse generator (Hewlett-Packard, HP 8082A) was connected to the other input. The pulse generator was triggered by the output of a second photodiode (EG&G, FND 100 Q) which was illuminated by a fraction of the light from the laser. Thereby, the gate was synchronized with the laser pulses, as the APD signal was only propagated through the gate when the output of the pulse generator was high. The delay and width of the gating pulse could be varied by changing the width and time delay of the square pulse from the frequency generator. For the data discussed in this paper, the delay was set such that the gating pulse always began with the laser pulse and was not varied. The output signal of the AND gate was stretched to 10 ns for data collection in the computer.

Autocorrelation analysis. Below, we present a brief account of the theoretical background of FCS, focusing on the case of multiple species. More details can be found in the literature.[5,14,16] The observed fluorescence intensity for two-photon excitation is given by the sum over all

fluorescent species:

$$F(t) = \frac{1}{2}\sum_{j=1}^{n} \kappa_j \sigma_j Q_j \int \mathrm{d}\mathbf{r} W(\mathbf{r}) C_j(\mathbf{r},t) \qquad (1)$$

where κ_j is the detection efficiency of species j, which depends on the spectral response of the detection system to the fluorescence emission, σ_j is the two-photon absorption cross-section at the wavelength of excitation and Q_j is the fluorescence quantum yield. The concentration, $C_j(\mathbf{r},t)$, is a function of both space and time because of the dynamic processes present in the sample (e.g. diffusion or chemical reactions). $W(\mathbf{r})$ denotes the product of the squared excitation intensity distribution, the extent of the sample and the emission intensity distribution measured at the detector and, thus, quantifies the spatial variation in the detected yield of photons from the excitation volume.

The fluorescence intensity fluctuates in time, and correlations in the fluctuations can be uncovered by calculating the intensity autocorrelation function, $G(\tau)$, defined as

$$G(\tau) = \frac{\langle F(t)F(t+\tau)\rangle - \langle F(t)\rangle^2}{\langle F(t)\rangle^2} \qquad (2)$$

where $\langle\ \rangle$ denotes the time average.

The function $W(\mathbf{r})$ is often treated as a three-dimensional Gaussian. For pure diffusion of n non-interacting species in a three-dimensional Gaussian excitation volume with radial dimension w_r (denoting the distance over which the intensity decays by a factor $1/e^2$) and axial dimension w_z, $G(\tau)$ can be calculated analytically from Eqns (1) and (2) and is given by

$$G(\tau) = \sum_{j=1}^{n} \mathscr{I}_j^2 G_{D_j}(\tau, N_j, \tau_{D_j}) \qquad (3)$$

which is the sum over the diffusion autocorrelation functions of all species j, G_{D_j}:

$$G_{D_j}(\tau, N_j, \tau_{D_j}) = \frac{\gamma}{\langle N_j\rangle}\left(\frac{1}{1+\tau/\tau_{D_j}}\right) \times \left[\frac{1}{1+(w_r/w_z)^2\tau/\tau_{D_j}}\right]^{1/2} \qquad (4)$$

weighted by the square of the fractional intensity contribution of species j:

$$\mathscr{I}_j = \frac{\kappa_j \sigma_j Q_j \langle C_j\rangle}{\sum_{k=1}^{n} \kappa_k \sigma_k Q_k \langle C_k\rangle} \qquad (5)$$

In Eqn. (4), $\gamma = (1/2)^{3/2}$ is a normalization factor and $\langle N_j\rangle$ is the average number of molecules of type j in the excitation volume. The diffusion time, τ_{D_j}, in the case of two-photon excitation is given by $\tau_{D_j} = w_r^2/8D_j$, with D_j representing the diffusion coefficient of molecules of type j.

In the presence of a chemical reaction, the species can interconvert, and the spatio-temporal evolution of the concentration, $C_j(\mathbf{r},t)$, is governed by the reaction–diffusion differential equation

$$\frac{\partial}{\partial t} C_j(\mathbf{r},t) = D_j \nabla^2 C_j(\mathbf{r},t) + \sum_{k=1}^{n} T_{jk} C_k(\mathbf{r},t) \qquad (6)$$

where T_{jk} is a matrix of the kinetic coefficients and n is the number of species that are involved in the reaction. Even for two interacting species, Eqn. (6) has no general analytical solution. In this paper, we limit ourselves to the special case of a bimolecular reaction of a small ligand L with a macromolecule M:

$$M + L \underset{k_b}{\overset{k_f}{\rightleftharpoons}} ML \qquad (7)$$

so that changes in the diffusion coefficient of the macromolecule upon ligand binding can be neglected, and hence $D_M = D_{ML} = D$. Moreover, under pseudo-first-order conditions with an abundance of ligand, $\langle C_L\rangle \gg \langle C_M\rangle$, the autocorrelation function can be calculated in closed form without any further approximations and is given by

$$G(\tau) = G_D(\tau, N_M + N_{ML}, \tau_D) \times \left[(\mathscr{I}_M + \mathscr{I}_{ML})^2 + K\langle C_L\rangle\left(\mathscr{I}_M - \frac{\mathscr{I}_{ML}}{K\langle C_L\rangle}\right)^2 e^{-\lambda\tau}\right] + G_{D_L}(\tau, N_L, \tau_{D_L})\mathscr{I}_L^2 \qquad (8)$$

Here, $\lambda = k_f\ (\langle C_M\rangle + \langle C_L\rangle) + k_b$ is the apparent rate coefficient of the reaction and $K = k_f/k_b$ is the equilibrium coefficient. The presence of a reaction appears as a relaxation process on top of the diffusional autocorrelation. It is evident that only those reactions can be studied where these additional correlations appear before the diffusional correlations have decayed. Because of the different diffusion coefficients, the equation is not symmetric with respect to ligands and macromolecules, and it is not possible to calculate the autocorrelation function for an excess of macromolecules in closed form without making additional assumptions.

RESULTS AND DISCUSSION

The effectiveness of the gating technique for measurements in a sample with background fluorescence was demonstrated with a mixture of 10 nM TMR and 25 μM

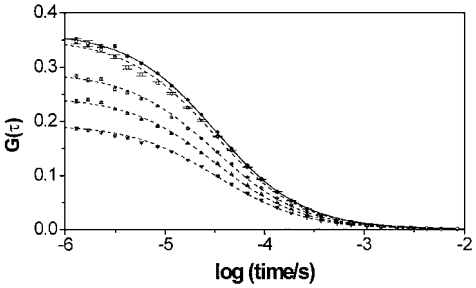

Figure 2. Intensity autocorrelation data and fits with Eqns (3) and (4) of 10 nM TMR (symbols and solid line) and a dye mixture of 10 nM TMR and 25 μM ANS at four different widths of the gating pulse (symbols and dashed lines; from bottom to top: no gate, 0.3 ns, 0.9 ns, 1.4 ns), plotted versus the logarithm of time in seconds

ANS where each species had a similar fluorescence intensity. The fluorescence lifetime of TMR is 2.2 ns, whereas the lifetime of ANS in aqueous buffer is less than 100 ps.[17] With this sample, the TMR fluorescence is observed in a background from a large number of weakly fluorescent ANS molecules. In Fig. 2, autocorrelation functions from this mixture are shown for various gate widths. For comparison, we also show the autocorrelation function of a 10 nM TMR sample without ANS. In the latter case, we obtain a simple diffusion autocorrelation function, characterized by a time constant $\tau_D = 32 \pm 1$ μs, and a fluctuation amplitude of 0.36, reflecting the fact that, according to Eqn. (4), one molecule resided in our excitation volume on the average. By adding ANS to the solution, more fluorescent molecules are in the excitation volume on average and, consequently, the fluctuation amplitude decreases. Note that the amplitude only drops by a factor of ~2, although the number of molecules increases about 1000-fold. This is a consequence of the much weaker fluorescence intensity per molecule of ANS compared with TMR and the fact that, according to Eqn. (3), the relative contributions are weighted by the square of the fractional intensities. By suppressing the fluorescence within the first 900 ps after the excitation pulse, the autocorrelation amplitude increases to 0.23, indicating that the background fluorescence from the ANS enters the measured autocorrelation function with a much smaller contribution. As we increase the gate width, the autocorrelation curve approaches the one of the TMR-only sample.

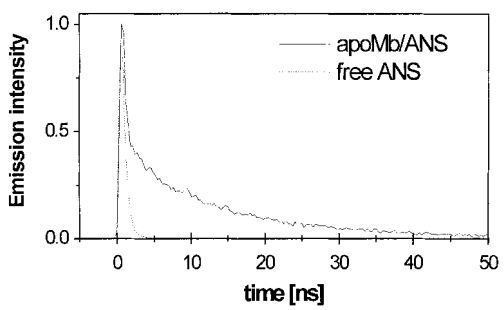

Figure 3. Normalized emission intensity of free ANS (dashed line) and a mixture of free and apoMb-bound ANS (solid line) in aqueous buffer plotted as a function of time

The gating circuit also proved useful in studies of the binding reaction of ANS to apoMb. Whereas ANS is only poorly fluorescent in solution, its fluorescence increases over 100-fold when it binds to the interior, hydrophobic regions of proteins. Concomitantly, the fluorescence lifetime increases enormously. Figure 3 shows the intensity of ANS in water and in solution with apomyoglobin as a function of the arrival time of the photons after the excitation pulse. Whereas the intensity decay of free ANS is faster than the time resolution of our system, the protein-bound ANS shows a much slower decay with a lifetime of 12.4 ± 0.2 ns. This pronounced sensitivity of ANS to its environment makes it an excellent probe for studies of protein stability and dynamics.[17]

Figure 4a shows the fluorescence autocorrelation function for dye-labeled myoglobin (diffusion only) and for the apoMb–ANS sample (diffusion and reaction) described in the Experimental section. These data were taken with the excitation beam diameter reduced from 5 to 3 mm. This underfilling of the back aperture of the objective increases the effective sample volume and thereby the diffusion correlation time. A gate width of ~2 ns was used for measuring the apoMb–ANS sample which efficiently suppressed the entire free ANS contribution to the autocorrelation function, as is evident in Fig. 3. In this case, the mathematical expression for the

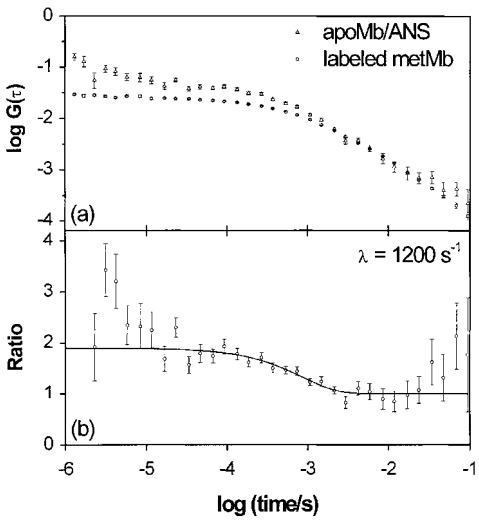

Figure 4. (a) Double-logarithmic plot of the intensity autocorrelation functions of apoMb in the presence of 1 μM ANS (diamonds), taken with the gate width of 2 ns to suppress the fluorescence contribution from free ANS, and of fluorescently labeled Mb (circles). The former autocorrelation function was scaled to compensate for the difference in protein concentration between the two samples. (b) Ratio of the two data sets plotted in (a), including the fit with the reaction term of Eqn. (9) as a solid line

autocorrelation function, Eqn. (8), simplifies to

$$G(\tau) = G_D(\tau, N_M + N_{ML}, \tau_D)\left[1 + \frac{1}{K\langle C_L\rangle}e^{-\lambda\tau}\right] \quad (9)$$

Equation (9) shows that the diffusion part can be removed when taking the ratio of the two correlation functions in Fig. 4(a), which leaves us with the reaction term (apart from a scaling factor). This ratio is plotted in Fig. 4(b). The process observed on time-scales less than 10 μs can be attributed to afterpulsing of the APD detector. The step seen in the millisecond time range represents the relaxation process due to the ligand binding reaction. Note that this reaction is less than ideal for FCS studies because the reaction occurs on a similar time-scale as diffusion and is therefore not easily detected in the apoMb–ANS FCS trace in Fig. 4(a). By fitting the data in Fig. 4(b), both the apparent rate coefficient $\lambda = 1200\ s^{-1}$ and the equilibrium coefficient $K = 1.1\ \mu M^{-1}$ were determined. The latter value for horse heart apoMb is similar to the one determined for ANS binding to sperm whale apoMb, $K = 0.3\ \mu M^{-1}$.[18] Assuming pseudo-first-order conditions and thus neglecting the protein concentration and the concentration of bound ligands in the expression for λ, we obtain $k_f = 620\ \mu M^{-1}\ s^{-1}$ and $k_b = 560\ s^{-1}$ for the microscopic rate coefficients. One could argue that the condition of excess ligand is not met because our experiments were done with 300 nM apoMb and 1 μM ANS. However, in the nanomolar concentration range, protein adsorption to the walls of our sample holder becomes significant, and so one expects that the fraction of apoMb in solution is much less. With the apparent rate coefficient λ, equilibrium constant K, ligand concentration $\langle C_L\rangle$ and diffusion time τ_D known, we fitted the autocorrelation function, Eqn. (9), to the data, with the average number of protein molecules in the sample volume, $N_M + N_{ML}$, as the only free parameter. In this case, a number corresponding to a total concentration of apoMb of 70 nM was obtained, and hence the pseudo-first-order assumption is well fulfilled.

CONCLUSIONS

Gating of the detected quanta in FCS experiments with pulsed excitation can be implemented with simple electronic circuitry. Here we have shown that this technique can be used to reject unwanted background and to simplify markedly the analysis of chemical reactions using FCS. Despite the overlap of reaction and diffusion time scales, both equilibrium and kinetic coefficients could be determined in a straightforward manner. While our approach convinces through being conceptually simple but powerful, a more elaborate version involves storing the arrival time after the excitation pulse for every counted photon, allowing more flexibility in the data analysis. Implementations of this approach have already been reported.[11]

Acknowledgments

We thank Karin Nienhaus and Uwe Theilen for help with the sample preparation. D. C. Lamb thanks the University of Ulm for a travel grant. This paper was written while G. U. Nienhaus was on sabbatical leave at Stanford University, supported by the Stiftung Volkswagenwerk. We also acknowledge support by the Graduiertenkolleg 328.

REFERENCES

1. Eigen M, Rigler R. *Proc. Natl. Acad. Sci. USA* 1994; **91**: 5740–5747.
2. Maiti S, Haupts U, Webb WW. *Proc. Natl. Acad. Sci. USA* 1997; **94**: 11753–11757.
3. Magde D, Elson EL. Webb WW. *Biopolymers* 1974; **13**: 29–61.
4. Ehrenberg M, Rigler R. *Chem. Phys.* 1974; **4**: 390–401.
5. Elson EL, Madge D. *Biopolymers* 1974; **13**: 1–27.
6. Magde D. *Q. Rev. Biophys.* 1976; **9**: 35–47.
7. Rauer B, Neumann E, Widengren J, Rigler R. *Biophys. Chem.* 1996; **58**: 3–12.
8. Widengren J, Rigler R, Mets Ü. *J. Fluorescence* 1994; **4**:255–258.
9. Widengren J, Mets Ü, Rigler R. *J. Phys. Chem.* 1995; **99**: 13368–13379.
10. Bonnet G, Krichevsky O, Libchaber A. *Proc. Natl. Acad. Sci. USA* 1998; **95**: 8602–8606.
11. Eggeling C, Fries JR, Brand L, Günther R, Seidel CAM. *Proc. Natl. Acad. Sci. USA* 1998; **95**: 1556–1561.
12. Chen Y, Müller JD, So PTC, Gratton E. *Biophys. J.* 1999; **77**: 553–567.
13. Kask P, Palo K, Ullmann D, Gall K. *Proc. Natl. Acad. Sci. USA* 1999; **96**: 13756–13761.
14. Thomson NL. In *Topics in Fluorescence Spectrocopy*, Volume 1: *Techniques*, Lakowicz JR (ed). Plenum Press: New York, 1991; 337–378.
15. Goeppert-Mayer M. *Ann. Phys.* 1931; **9**: 273–295.
16. Aragón SR, Pecora R. *J. Chem. Phys.* 1976; **64**: 1791–1803.
17. Bismuto E, Irace G, Sirangelo I, Gratton E. *Protein Sci.* 1996; **5**: 121–126.
18. Stryer L. *J. Mol. Biol.* 1965; **13**: 482–495.

